UTILIZING SMALL QUANTUM COMPUTERS FOR MACHINE LEARNING AND GROUND STATE ENERGY APPROXIMATION

Stian Bilek

Department of Physics University of Oslo Oslo, Norway stian.bilek@fys.uio.no

July 26, 2024

ABSTRACT

Quantum circuit partitioning (QCP) is a hybrid quantum-classical approach that aims to simulate large quantum systems on smaller quantum computers. A quantum computation is divided into smaller subsystems and results of measurements on these subsystems are combined using classical processing. In this paper, we propose a QCP strategy to measure an observable on a large quantum system by utilizing several quantum systems of smaller size. The method can be applied to both machine learning and variational ground state energy approximation, and we show that the required calculations and the variance of the gradients can be tailored to scale efficiently with the total number of qubits. Thus it can be utilized to mitigate the well-known problem of barren plateaus. Additionally, the method can be realized by performing simple measurements of Pauli-strings on the separate subsystems, and the gradients can be estimated with common methods such as the parameter-shift rule. We demonstrate the method by approximating the ground state energy of the 1D transverse-field Ising model with periodic boundary conditions, and by classifying handwritten digits. For the ground state energy approximation, we achieved a relative error within the order of 0.1% for all the tested systems sizes. When applied to the classification between the digits 3 and 6, we were able to generalize to out-of-sample data with 100% accuracy.

Contents

3 Method

1	oduction	2						
2	Theory							
	2.1	Quantum states and observables	3					
	2.2	Supervised learning	2					
		2.2.1 Gradients	4					
		2.2.2 Computational complexities	4					
	2.3	Variational quantum eigensolvers	6					
		2.3.1 Gradients	6					
		2.3.2 Computational complexities and the choice of Pauli-strings	7					
	2.4	Barren plateaus	7					

10

5	Con	clusion		14	
	4.2	Superv	ised learning	13	
	4.1	Ground	l state energy	12	
4	Resu			12	
		3.2.3	Observable	12	
		3.2.3	Observable		
		3.2.2	Ansatz	11	
		3.2.1	Dataset	11	
	3.2	Superv	ised learning	11	
		3.1.3	Global unitary	10	
		3.1.2	Subsystem unitaries	10	
		3.1.1	The Hamiltonian	10	
	3.1	1 Ground state energy			

1 Introduction

Quantum computers have the potential to solve certain problems that are intractable for classical computers by exploiting the unique properties of quantum mechanics [1] [2]. Consequently, there has been an increasing interest in employing quantum computers in machine learning tasks to explore whether they can provide a competitive edge in this domain. Indeed, several quantum algorithms such as Quantum Support Vector Machines [3], Quantum Principal Component Analysis [4], Quantum Nearest-Neighbor Classification [5] and Quantum Principal Component Analysis [4] offer speed-ups over their classical analogue under certain assumptions.

However, the current noisy intermediate scale quantum (NISQ) era of quantum computing poses several challenges for the practical implementation of quantum algorithms [6]. We have limitations in the decoherence-times, the number of available qubits, the accuracy of quantum gates and also the connectivity between qubits. Practical demonstrations of quantum speed-ups in the NISQ era are thus reliant on algorithms that respects these hardware limitations. In this regard, new and promising methods specifically tailored for NISQ devices have been developed, such as employing parameterized quantum circuits (PQC) [7] for machine learning.

A central part of the PQC method is the way which the data set is encoded into the quantum state of the quantum computer. While classical computers can handle very large data sets and complex models, the relatively short coherence times of NISQ devices restricts the possible ways for which data sets can be encoded reliably. A currently popular encoding scheme is thus to embed each feature of the data set into a respective qubit with the application of single qubit rotations [7]. While the circuit depth of this approach scales as $\mathcal{O}(1)$, the qubit requirement scales linearly in the number of data set features p, thus limiting the data sets for which this can be done reliably.

To address this limitation, one promising approach is to use a divide and conquer strategy, which involves breaking down a large problem into smaller, more manageable subproblems that can be solved independently and then combined to obtain the overall solution. This strategy has been widely used in classical computing for tasks such as sorting [8], geometric intersection problems [9], and matrix multiplication [10]. In the context of quantum computing, Quantum circuit partitioning (QCP) is a hybrid quantum-classical approach with the goal of utilizing small quantum computers to simulate larger quantum systems. The idea is to partition large quantum circuits into smaller parts that can be run on a smaller quantum computer than the original circuit. These smaller circuits are measured, before combining the measurement results using classical resources to emulate the full circuit. Several studies have explored this task from different angles. Bravyi et al. showed that any (n+k)-qubit circuit where each qubit participates in at most d two-qubit gates (d-sparse circuits), can be simulated on an n-qubit device with classical processing in $2^{\mathcal{O}(kd)}$ poly(n) steps [11]. Due to the exponential scaling in k and d, this methods practicality is arguably dependent on these parameters being small. Fujii et al. utilized a similar approach applied to VQE in order to estimate the ground state energy of one-dimensionally coupled Heisenberg antiferromagnetic models on kagome lattices as well as two-dimensional Heisenberg antiferromagnetic models on square lattices [12]. Their method is reliant on weak-interactions between circuit partitions, along with subroutines such as the estimation of inner products between quantum states and the Gram-Schmidt procedure. In the context of quantum machine learning, QCP has been applied to to digit recognition

[13], where they successfully applied quantum computers much smaller than the data dimension. This method is also reliant on the estimation of inner products between quantum states. For a specific family of quantum circuits and observables, QCP has also been shown to mitigate the problem of barren plateaus [14], a current obstacle for many practical quantum computing algorithms. However, the specific family of quantum models they consider does not allow observables that measure qubits in two partitions simultaneously. All though the work done on QCP in this thesis shares similarities with the referenced work, it is aimed at mitigating some of the potential drawbacks of present methods. It allows for a subexponential scaling even as the target system size increases, it is not dependent on any inner product estimations, and it allows for interactions or measurements that act across circuit partitions. The problem of barren plateus can also be mitigated with our approach. Moreover, it can be applied both for machine learning and variational quantum eigensolver tasks. However, the mitigation of these drawbacks does come at the cost of a limitation on the applicable quantum circuits.

The study is structured as follows: Section 2 details the theory behind the approach and explains how it can be utilized for both ground state approximation and machine learning tasks. In addition, we show in the final subsection that the problem of barren plateaus can be mitigated. In section 3 we detail the specific problems we apply our method on, and show how the method is set up. In section 4, we present and discuss the results of our simulations, while we finally conclude and discuss future work in section 5.

2 Theory

2.1 Quantum states and observables

Before discussing the specific method, it will help to define what is meant by local operators. We say that an operator is local to a specific subset of the qubits if it acts non-trivially only on said subset, but trivially on all qubits outside of the subset. A trivial operation to a qubit is simply the identity operation $\hat{A} | \psi \rangle = | \psi \rangle$. For example, the four-qubit operator $B = I \otimes X \otimes Y \otimes I + I \otimes I \otimes I \otimes X$ only acts trivially on the first qubit, hence it is local to the second, third and fourth qubit.

The aim of the following method is to estimate expectation values of an n-qubit state $|\psi\rangle$ with respect to some measurement operator M, that is $\langle \psi | M | \psi \rangle$, by utilizing less than n qubits. We start out with an n-qubit system in the ground state and partition these n qubits into S subsystems $\bigotimes_{s=1}^S |0\rangle_s$. The number of qubits in each subsystem, denoted n_s , is arbitrary as long as $\sum_{s=1}^S n_s = n$. The next step is to apply a tensor product of unitary operations local to each partition, which allows us to express our quantum state as $\bigotimes_{s=1}^S U_s |0\rangle_s$. Finally, we apply an arbitrary global unitary V to the full system resulting in the state,

$$|\psi\rangle = V \bigotimes_{s=1}^{S} U_s |0\rangle_s. \tag{1}$$

The measurement operators we will consider are Pauli strings of the form $M_m = \sigma_i^m \otimes \sigma_j^m \otimes \cdots \otimes \sigma_k^m$, with $\sigma_i^m \in \{I, \sigma_x, \sigma_y, \sigma_z\}$, but our results can easily be extended to general operators $M = \sum_m d_m M_m$ due to the linearity of expectation values with respect to a sum of operators. We are thus interested in the quantity,

$$\langle \psi | M_m | \psi \rangle = \left[\bigotimes_{s=1}^{S} \langle 0 |_s U_s^{\dagger} \right] V^{\dagger} M_m V \bigotimes_{s=1}^{S} U_s | 0 \rangle_s.$$
 (2)

We can rewrite this expectation value by expressing the global unitary as $V=\sum_l \lambda_l \sigma_p^l \otimes \sigma_q^l \otimes \cdots \otimes \sigma_r^l$, as long as the coefficients λ^l are chosen to ensure unitarity. We have

$$\langle \psi | M_{m} | \psi \rangle = \sum_{l} \sum_{l'} \lambda_{l}^{*} \lambda_{l'}$$

$$[\bigotimes_{s=1}^{S} \langle 0|_{s} U_{s}^{\dagger}] [\sigma_{p}^{l} \otimes \sigma_{q}^{l} \otimes \cdots \otimes \sigma_{r}^{l}] [\sigma_{i}^{m} \otimes \sigma_{j}^{m} \otimes \cdots \otimes \sigma_{k}^{m}] [\sigma_{p'}^{l} \otimes \sigma_{q'}^{l} \otimes \cdots \otimes \sigma_{r'}^{l}] \bigotimes_{s=1}^{S} U_{s} |0\rangle_{s}$$

$$= \sum_{l} \sum_{l'} \lambda_{l}^{*} \lambda_{l'} [\bigotimes_{s=1}^{S} \langle 0|_{s} U_{s}^{\dagger}] [\sigma_{p}^{l} \sigma_{i}^{m} \sigma_{p'}^{l} \otimes \sigma_{q}^{l} \sigma_{j}^{m} \sigma_{q'}^{l} \otimes \cdots \otimes \sigma_{r}^{l} \sigma_{k}^{m} \sigma_{r'}^{l}] \bigotimes_{s=1}^{S} U_{s} |0\rangle_{s}$$

$$= \sum_{p} d_{p} [\bigotimes_{s=1}^{S} \langle 0|_{s} U_{s}^{\dagger}] [\sigma_{i}^{p} \otimes \sigma_{j}^{p} \otimes \cdots \otimes \sigma_{k}^{p}] \bigotimes_{s=1}^{S} U_{s} |0\rangle_{s}$$

$$= \sum_{p} d_{p} \prod_{s=1}^{S} \langle 0|_{s} U_{s}^{\dagger} W_{s}^{p} U_{s} |0\rangle_{s},$$

$$(4)$$

(5)

where d_p are complex coefficients and W^p_s are tensor products of Pauli-operators local to subset s. Going from Eq. 3 to Eq. 4, we utilized the fact that a product of Pauli-operators can be written as $\sigma_a \sigma_b \sigma_c = e^{i\alpha} \sigma_d$, allowing us to re-express the observable in Eq. 3 as $\sum_l \sum_{l'} \lambda^*_l \lambda_l [\sigma^l_p \sigma^m_i \sigma^l_{p'} \otimes \sigma^l_q \sigma^m_j \sigma^l_{q'} \otimes \cdots \otimes \sigma^l_r \sigma^m_{r'}] = d_p [\sigma^p_i \otimes \sigma^p_j \otimes \cdots \otimes \sigma^p_k] = \frac{1}{2} \sum_{l'} \frac{1}{2} \sum_{l'} \lambda^*_l \lambda_l [\sigma^l_p \sigma^m_i \sigma^l_{p'} \otimes \sigma^l_q \sigma^m_j \sigma^l_{q'} \otimes \cdots \otimes \sigma^l_r \sigma^m_{r'}] = d_p [\sigma^p_i \otimes \sigma^p_j \otimes \cdots \otimes \sigma^p_k] = \frac{1}{2} \sum_{l'} \frac{1}{2} \sum_{l'} \lambda^*_l \lambda_l [\sigma^l_p \sigma^m_i \sigma^l_{p'} \otimes \sigma^l_q \sigma^m_j \sigma^l_{q'} \otimes \cdots \otimes \sigma^l_r \sigma^m_{r'}] = d_p [\sigma^p_i \otimes \sigma^p_j \otimes \cdots \otimes \sigma^p_k]$ $\sum_{p} d_{p} \bigotimes_{s=1}^{S} W_{s}^{p}$. The key takeaway from Eq. 5 is that we are able to express the expectation value on the full n-qubit system in Eq. 2 in terms of products of measurements on the S subsystems. Even so, the practicality of the method relies on the scaling of the number of expectation values and complex coefficients in the number of qubits. We will

discuss this along with how we can apply Eq. 5 for machine learning tasks and VQE tasks in the upcoming sections.

2.2 **Supervised learning**

In this section, we will show how the expectation value in Eq. 2 can be utilized for supervised learning tasks on quantum computers with less qubits than in the original quantum state. Assume that a sample of our dataset features is given by $\vec{x} \in \mathbb{R}^p$. A common way to encode these p features into a quantum state is to embed each feature into a respective qubit with the application of single qubit rotations [7]. This task requires a quantum computer of at least p qubits. If only an m < p-qubit quantum computer is available, we divide the features into S subsets of at most size m, denoted $\vec{x}^{(s)}$ for $s = 1, 2, \dots, S$.

First, we rewrite the quantum state in Eq. 1 as

$$|\psi\rangle = V \bigotimes_{s=1}^{S} U_{s}(\vec{x}^{(s)}, \theta_{1}^{(s)}, \theta_{2}^{(s)}, \dots) |0\rangle_{s},$$

where $\theta_i^{(s)}$ is the i'th rotational parameter for subset s. For many machine learning tasks, the models predictions does not need to associate with the measurement of an hermitian operator M_m on a normalized quantum state $V \bigotimes_{s=1}^S U_s |0\rangle_s$. This means that the observable $\sum_p d_p \bigotimes_{s=1}^S W_s^p$ in Eq. 5 can be chosen arbitrarily, for example as a linear combination of some n-qubit Pauli strings. Given $\sum_{n} d_{p} \bigotimes_{s=1}^{S} W_{s}^{p}$ of such form, we use eq. 5 and define our quantum model as

$$f(\vec{x}, \theta_1^{(1)}, \theta_2^{(1)}, \dots, \theta_1^{(2)}, \theta_2^{(2)}, \dots, d_1, d_2, \dots) = \sum_{p} d_p \prod_{s=1}^{S} \langle 0|_s U_s^{\dagger}(\vec{x}^{(s)}, \theta_1^{(s)}, \theta_2^{(s)}, \dots) W_s^p U_s(\vec{x}^{(s)}, \theta_1^{(s)}, \theta_2^{(s)}, \dots) |0\rangle_s.$$
 (6)

This expression, or some classical processing step, $g[f(\vec{x}, \theta_1^{(1)}, \theta_2^{(1)}, \dots, \theta_1^{(2)}, \theta_2^{(2)}, \dots, d_1, d_2, \dots)]$, gives us the output of our supervised model.

2.2.1 Gradients

Given a differentiable loss function, training supervised models with gradient descent methods require calculating the partial derivatives of the expression in Eq. 6, wrt. the trainable parameters of our model. For the coefficients, we have

$$\frac{\partial f(\vec{x}, \theta_1^{(1)}, \theta_2^{(1)}, \dots, \theta_1^{(2)}, \theta_2^{(2)}, \dots, d_1, d_2, \dots)}{\partial d_q} = \prod_{s=1}^{S} \langle 0|_s U_s^{\dagger}(\vec{x}^{(s)}, \theta_1^{(s)}, \theta_2^{(s)}, \dots) W_s^q U_s(\vec{x}^{(s)}, \theta_1^{(s)}, \theta_2^{(s)}, \dots) |0\rangle_s,$$
(7)

which is straight forward to evaluate. For the rotational parameters, we have

$$\frac{\partial f(\vec{x}, \theta_{1}^{(1)}, \theta_{2}^{(1)}, \dots, \theta_{1}^{(2)}, \theta_{2}^{(2)}, \dots, d_{1}, d_{2}, \dots)}{\partial \theta_{i}^{(q)}} = \sum_{p} d_{p} \frac{\partial}{\partial \theta_{i}^{(q)}} \left(\langle 0 |_{q} U_{q}^{\dagger}(\vec{x}^{(q)}, \theta_{1}^{(q)}, \theta_{2}^{(q)}, \dots) W_{q}^{p} U_{q}(\vec{x}^{(q)}, \theta_{1}^{(q)}, \theta_{2}^{(q)}, \dots) | 0 \rangle_{q} \right) \\
\cdot \prod_{s \neq q} \langle 0 |_{s} U_{s}^{\dagger}(\vec{x}^{(s)}, \theta_{1}^{(s)}, \theta_{2}^{(s)}, \dots) W_{s}^{p} U_{s}(\vec{x}^{(s)}, \theta_{1}^{(s)}, \theta_{2}^{(s)}, \dots) | 0 \rangle_{s}, \tag{8}$$

where

$$\frac{\partial}{\partial \theta_{\cdot}^{(q)}} \left(\langle 0 |_{q} U_{q}^{\dagger}(\vec{x}^{(q)}, \theta_{1}^{(q)}, \theta_{2}^{(q)}, \dots) W_{q}^{p} U_{q}(\vec{x}^{(q)}, \theta_{1}^{(q)}, \theta_{2}^{(q)}, \dots) | 0 \rangle_{q} \right)$$
(9)

can be evaluated with the parameter-shift rule [15].

2.2.2 Computational complexities

As mentioned earlier, the observable $\sum_p d_p \bigotimes_{s=1}^S W_s^p$ can be chosen arbitrarily for many machine learning tasks. If chosen as a linear combination of all possible n-qubit Pauli strings, the maximum number of expectation values for subsystem s is given by the number of unique combinations of the Pauli-basis, $\{I, X, Y, Z\}$, on n_s qubits, that is 4^{n_s} . The total number of expectation values is therefore at most $\sum_{s=1}^S 4^{n_s}$. One can show that this number can be made polynomial in the number of qubits n. If we partition the system into $S = n/n_s$ equally sized subsystems of $n_s = \beta \log_2(n)$ qubits, for some constant β , the total number of expectation values is given by

$$n_E \le S \cdot 4^{n_s} = \frac{n}{\beta \log_2(n)} 2^{2\beta \log_2(n)} = \frac{n^{2\beta+1}}{\beta \log_2(n)}.$$

Despite the polynomial scaling of the number of expectation values, we still require one coefficient d_p for every possible n-qubit combination of the Pauli-basis. The scaling in the number of coefficients is hence 4^n . However, one could evaluate all the required expectation values in polynomial time, and then make an informed choice of a number of terms from Eq. 6 polynomial in n. One approach is to evaluate the gradients in Eq. 9 and chose to form $\sum_p d_p \bigotimes_{s=1}^S W_s^p$ as a combination of the Pauli-strings W_s^p which provided the gradient with the largest magnitude. Another approach can be seen by inspecting Eq. 7. We see from this equation that the rate of change of the expectation value wrt. the coefficients is proportional to products of expectation values on each subsystem. Further, for a given loss function $L(g[f(\vec{\phi})])$, the gradient wrt. the parameter ϕ_i is given by

$$\frac{\partial L(g[f(\vec{\phi})])}{\partial \phi_i} = \frac{\partial L(g[f(\vec{\phi})])}{\partial g[f(\vec{\phi})]} \frac{\partial g[f(\vec{\phi})]}{\partial f(\vec{\phi})} \frac{\partial f(\vec{\phi})}{\partial \phi_i}.$$

When $f(\vec{\phi})$ is the expectation value in Eq. 6, it follows that products of expectation values which are close to zero will lead to a small factor in the rate of change of the loss function wrt. our coefficients. We thus evaluate all possible expectation values on all subsystems, and construct $\sum_p d_p \bigotimes_{s=1}^S W_s^p$ by combining operators W_s^p which resulted in expectation values with the largest magnitudes. If a polynomial in n such combinations are chosen, it follows that the number of coefficients is also polynomial in n.

We can also limit the number of terms in $\sum_p d_p \bigotimes_{s=1}^S W_s^p$ by considering it as a linear combination of up to p-qubit operators, where p < n. The number of ways to chose p qubits from n qubits is $\binom{n}{p}$, and there are 4^p ways to combine the Pauli-basis for each of these combinations. Thus the number of coefficients required is $\sum_{k=1}^p \binom{n}{k} 4^k$. We can utilize the upper bound $\binom{n}{k} \leq (\frac{en}{k})^k$ to rewrite this as $n_T \leq = \sum_{k=1}^p (\frac{en}{k})^k 4^k$. For fixed p and large n, the term with the highest power, $(\frac{en}{p})^p 4^p$, grows the fastest. This results in an asymptotical complexity of $\mathcal{O}(n^p)$.

2.3 Variational quantum eigensolvers

Given a Hamiltonian $H = \sum_m \lambda_m M_m$, where λ_i are real coefficients and M_m are Pauli-strings, the aim with VQE is to minimize the energy,

 $E = \left\langle \psi(\vec{\phi}) \middle| H \middle| \psi(\vec{\phi}) \right\rangle,\,$

by varying the parameters $\vec{\phi}$. Instead of measuring H directly on the state $|\psi\rangle = V \bigotimes_{s=1}^S U_s(\vec{\theta_s}) |0\rangle_s$, our method relies on measurements of the products $V^\dagger H V$ on the state $\bigotimes_{s=1}^S U_s(\vec{\theta_s}) |0\rangle_s$. For $V = \sum_i c_i P_i$, we can according to Eq. 2 write out the energy expression as

$$E(\theta_{1}^{(1)}, \theta_{2}^{(1)}, \dots, \theta_{1}^{(2)}, \theta_{2}^{(2)}, \dots, c_{1}, c_{2}, \dots) = \left[\bigotimes_{s=1}^{S} \langle 0|_{s} U_{s}^{\dagger}(\vec{\theta}_{s}) \right] V^{\dagger} H V \left[\bigotimes_{s=1}^{S} U_{s}(\vec{\theta}_{s}) |0\rangle_{s} \right]$$

$$= \sum_{p} d_{p}(c_{1}, c_{2}, \dots, \lambda_{1}, \lambda_{2}, \dots) \prod_{s=1}^{S} \langle 0|_{s} U_{s}^{\dagger}(\vec{\theta}_{s}) W_{s}^{p} U_{s}(\vec{\theta}_{s}) |0\rangle_{s}. \quad (10)$$

In order to utilize our approach for methods such as the variational quantum eigensolver (VQE), one is reliant on the unitarity of the operator V. Thus, the measurement of $V^{\dagger}M_mV = \sum_p d_p \bigotimes_{s=1}^S W_s^p$ will need to correspond to the measurement of the hermitian operator M_m on a normalized state $V \bigotimes_{s=1}^S U_s |0\rangle_s$. Since V is of dimensionality $2^n \otimes 2^n$, efficient construction of this unitary and calculation of the products $V^{\dagger}M_mV$ is not straight forward. However, by restricting the form of V this can be achieved efficiently. We first define a set of Pauli-strings $\{P_1, P_2, \ldots, P_N\}$ and real scalars $\{c_1, c_2, \ldots, c_N\}$. We then express V as,

$$V = \prod_{i=1}^{N} [\cos(c_i)I + i\sin(c_i)P_i]$$

$$= \prod_{i=1}^{N} \overline{P}_i.$$
(11)

This ensures the unitarity of V since

$$\overline{P}_i^{\dagger} \overline{P}_i = [\cos(c_i)I - i\sin(c_i)P_i][\cos(c_i)I + i\sin(c_i)P_i]$$
$$= \cos^2(c_i)I + \sin^2(c_i)I = I.$$

We will return to detailing the construction of the Pauli-strings and the scaling of Eq. 11 in section 2.3.2.

2.3.1 Gradients

We can minimize the energy expression in Eq. 10 by finding its gradient wrt. the rotational parameters, $\vec{\theta}_s$ and the coefficients, c_i . The rotational parameters follow a similar expression as for the supervised learning case, that is,

$$\frac{\partial E(\theta_{1}^{(1)}, \theta_{2}^{(1)}, \dots, \theta_{1}^{(2)}, \theta_{2}^{(2)}, \dots, c_{1}, c_{2}, \dots)}{\partial \theta_{i}^{(q)}} = \sum_{p} d_{p} \frac{\partial}{\partial \theta_{i}^{(q)}} \left(\langle 0 |_{q} U_{q}^{\dagger}(\theta_{1}^{(q)}, \theta_{2}^{(q)}, \dots) W_{q}^{p} U_{q}(\theta_{1}^{(q)}, \theta_{2}^{(q)}, \dots) | 0 \rangle_{q} \right) \\
\cdot \prod_{s \neq q} \langle 0 |_{s} U_{s}^{\dagger}(\vec{x}^{(s)}, \theta_{1}^{(s)}, \theta_{2}^{(s)}, \dots) W_{s}^{p} U_{s}(\vec{x}^{(s)}, \theta_{1}^{(s)}, \theta_{2}^{(s)}, \dots) | 0 \rangle_{s}, \tag{12}$$

where

$$\frac{\partial}{\partial \theta_{:}^{(q)}} \left(\langle 0|_{q} U_{q}^{\dagger}(\theta_{1}^{(q)}, \theta_{2}^{(q)}, \dots) W_{q}^{p} U_{q}(\theta_{1}^{(q)}, \theta_{2}^{(q)}, \dots) |0\rangle_{q} \right)$$

can be evaluated with the parameter-shift rule [15]. For the coefficients we have,

$$\frac{\partial E(\theta_1^{(1)}, \theta_2^{(1)}, \dots, \theta_1^{(2)}, \theta_2^{(2)}, \dots, c_1, c_2, \dots)}{\partial c_i} = \sum_{p} \frac{\partial d_p(c_1, c_2, \dots)}{\partial c_i} \prod_{s=1}^{S} \langle 0|_s U_s^{\dagger}(\vec{\theta}_s) W_s^p U_s(\vec{\theta}_s) |0\rangle_s, \tag{13}$$

where the products $\prod_{s=1}^{S} \langle 0|_{s} U_{s}^{\dagger}(\vec{\theta_{s}}) W_{s}^{p} U_{s}(\vec{\theta_{s}}) |0\rangle_{s}$ are already evaluated when producing the output.

2.3.2 Computational complexities and the choice of Pauli-strings

Expressing V as in Eq. 11 and expanding the product results in a sum of 2^N terms. The observable $V^{\dagger}M_mV$ will thus consist of 2^{2N} terms, and if $N=\beta\log_2(n)$, the total number of terms is $n^{2\beta}$. If a logarithmic in n number of Pauli-strings is not sufficient, we can restrict the choice of $\{P_1,P_2,\cdots,P_N\}$ in order to achieve a scaling independent of N.

We construct a set of Pauli strings $\{P_1, P_2, \cdots, P_N\}$ with specific non-commutation properties to achieve scaling independent of N, and we start with the assumption that P_{i_1} is the first Pauli string which is non-commutative with M_m . The target observable $V^{\dagger}M_mV$ can then be written as

$$V^{\dagger} M_m V = \overline{P_N}^{\dagger} \cdots \overline{P_{i_1}}^{\dagger} \cdots \overline{P_1}^{\dagger} M_m \overline{P_1} \cdots \overline{P_{i_1}} \cdots \overline{P_N}$$
$$= \overline{P_N}^{\dagger} \cdots \overline{P_{i_1}}^{\dagger} M_m \overline{P_{i_1}} \cdots \overline{P_N}.$$

Next, we identify the Pauli string P_{i_2} , which is the next Pauli string that is non-commutative with either P_{i_1} or M_m . We then have

$$\begin{split} V^{\dagger} M_m V &= \overline{P}_N^{\dagger} \cdots \overline{P}_{i_2}^{\dagger} \cdots \overline{P}_{i_1+1}^{\dagger} \overline{P}_{i_1}^{\dagger} M_m \overline{P}_{i_1} \overline{P}_{i_1+1} \cdots \overline{P}_{i_2} \cdots \overline{P}_N \\ &= \overline{P}_N^{\dagger} \cdots \overline{P}_{i_2}^{\dagger} \overline{P}_{i_1}^{\dagger} M_m \overline{P}_{i_1} \overline{P}_{i_2} \cdots \overline{P}_N. \end{split}$$

We can proceed similarly by finding the next Pauli string P_{i_3} , which is non-commutative with either M_m , P_{i_1} , or P_{i_2} , and then continue this process for the next Pauli string P_{i_4} . Assuming there exists a total of K such Pauli strings for M_m , we get

$$V^{\dagger} M_m V = \overline{P_{i_K}}^{\dagger} \cdots \overline{P_{i_2}}^{\dagger} \overline{P_{i_1}}^{\dagger} M_m \overline{P}_{i_1} \overline{P_{i_2}} \cdots \overline{P_{i_K}}.$$

This results in 2^{2K} expectation values per observable M_m , and is thus constant in n for fixed K. We can also allow K to scale with n by chosing $K = \beta \log_2(n)$, resulting in $n^{2\beta}$ terms per observable M_m .

Given a Hamiltonian of L terms, $H = \sum_{m=1}^L \lambda_m M_m$, the product $V^\dagger H V$ can be expanded to yield the new observable $D = V^\dagger H V = \sum_p d_p \bigotimes_{s=1}^S W_s^p$. By following the strategy outlined above, this observable will contain at most $L2^{2K}$ Pauli strings. The number of expectation values that has to be evaluated depends on H and the choice of the Pauli strings P_i . Worst case scenario is that every term in D acts on all the n qubits, requiring one expectation value per each of the S subsystems, per term. This results in $SL2^{2K}$ expectation values, which can be made subexponential in n as long as the Hamiltonian can be expressed with a number of terms L polynomial in n.

2.4 Barren plateaus

McClean et al. showed that for a wide range of parameterized circuits, the probability that a gradient along any direction being non-zero vanishes exponentially in the number of qubits [16]. This results in a significant challenge in the training of such quantum models, hence it is natural to explore the behaviour of the gradients for our method. We are interested in the variance of the partial derivatives for the supervised learning case in Eq. 8, and how these scale with n. We are thus interested in,

$$\operatorname{Var}\left[\frac{\partial f(\vec{x}, \theta_{1}^{(1)}, \theta_{2}^{(1)}, \dots, \theta_{1}^{(2)}, \theta_{2}^{(2)}, \dots, d_{1}^{(1)}, \dots)}{\partial \theta_{i}^{(q)}}\right] =$$

$$\operatorname{Var}\left[\sum_{p} d_{p} \frac{\partial}{\partial \theta_{i}^{(q)}} \left(\left\langle 0|_{q} U_{q}^{\dagger}(\vec{x}^{(q)}, \theta_{1}^{(q)}, \theta_{2}^{(q)}, \dots) W_{q}^{p} U_{q}(\vec{x}^{(q)}, \theta_{1}^{(q)}, \theta_{2}^{(q)}, \dots) |0\rangle_{q}\right)$$

$$\cdot \prod_{s \neq q} \left\langle 0|_{s} U_{s}^{\dagger}(\vec{x}^{(s)}, \theta_{1}^{(s)}, \theta_{2}^{(s)}, \dots) W_{s}^{p} U_{s}(\vec{x}^{(s)}, \theta_{1}^{(s)}, \theta_{2}^{(s)}, \dots) |0\rangle_{s}\right]$$

$$= \operatorname{Var}\left[\sum_{p} d_{p} R_{q}^{(p)} \prod_{s \neq q} B_{s}^{(p)}\right],$$

$$(14)$$

where

$$R_q^{(p)} = \frac{\partial}{\partial \theta_i^{(q)}} \left(\langle 0 |_q U_q^{\dagger}(\vec{x}^{(q)}, \theta_1^{(q)}, \theta_2^{(q)}, \dots) W_q^p U_q(\vec{x}^{(q)}, \theta_1^{(q)}, \theta_2^{(q)}, \dots) | 0 \rangle_q \right),$$

and

$$B_s^{(p)} = \langle 0|_s U_s^{\dagger}(\vec{x}^{(s)}, \theta_1^{(s)}, \theta_2^{(s)}, \dots) W_s^p U_s(\vec{x}^{(s)}, \theta_1^{(s)}, \theta_2^{(s)}, \dots) |0\rangle_s.$$

Since $R_q^{(p)}$ and $R_{q'}^{(p)}$ for $q \neq q'$ are measurements on different subsystems, we consider $R_q^{(p)}$ to be independent of all variables except $R_q^{(p')}$ for all p'. The same can be argued for $B_s^{(p)}$. Further we consider d_p to have zero mean, variance σ_d^2 and to be independent of all the other variables. We continue by utilizing that

$$\operatorname{Var}[\sum_{i} X_{i}] = \sum_{i} \operatorname{Var}[X_{i}] + 2 \sum_{i < j} \operatorname{Cov}[X_{i}, X_{j}],$$

which gives

$$\mathrm{Var}[\sum_{i} d_{i} R_{q}^{(i)} \prod_{s \neq q} B_{s}^{(i)}] = \sum_{i} \mathrm{Var}[d_{i} R_{q}^{(i)} \prod_{s \neq q} B_{s}^{(i)}] + 2 \sum_{i < j} \mathrm{Cov}[d_{i} R_{q}^{(i)} \prod_{s \neq q} B_{s}^{(i)}, d_{j} R_{q}^{(j)} \prod_{s \neq q} B_{s}^{(j)}].$$

First we deal with the covariance by utilizing Cov(X, Y) = E[XY] - E[X]E[Y], which gives,

$$\begin{split} \text{Cov}[d_{i}R_{q}^{(i)}\prod_{s\neq q}B_{s}^{(i)},d_{i}R_{q}^{(j)}\prod_{s\neq q}B_{s}^{(j)}] &= \text{E}[d_{i}R_{q}^{(i)}(\prod_{s\neq q}B_{s}^{(i)})d_{j}^{*}R_{q}^{(j)}\prod_{s\neq q}B_{s}^{(j)}]\\ &- \text{E}[d_{i}R_{q}^{(i)}\prod_{s\neq q}B_{s}^{(i)}]\text{E}[d_{j}^{*}R_{q}^{(j)}\prod_{s\neq q}B_{s}^{(j)}]\\ &= \text{E}[d_{i}]\text{E}[d_{j}^{*}]\text{E}[R_{q}^{(i)}R_{q}^{(j)}]\text{E}[(\prod_{s\neq q}B_{s}^{(i)})\prod_{s\neq q}B_{s}^{(j)}]\\ &- \text{E}[d_{i}]\text{E}[d_{j}^{*}]\text{E}[R_{q}^{(i)}]\text{E}[R_{q}^{(j)}]\text{E}[(\prod_{s\neq q}B_{s}^{(i)})]\text{E}[\prod_{s\neq q}B_{s}^{(j)}]\\ &= 0, \end{split}$$

since d_i has mean zero. We are then left with

$$\begin{split} \text{Var}[\sum_{i} d_{i}R_{q}^{(i)} \prod_{s \neq q} B_{s}^{(i)}] &= \sum_{i} \text{Var}[d_{i}R_{q}^{(i)} \prod_{s \neq q} B_{s}^{(i)}] \\ &= \sum_{i} \bigg(\text{E}[d_{i}R_{q}^{(i)} (\prod_{s \neq q} B_{s}^{(i)}) d_{i}^{*}R_{q}^{(i)} (\prod_{s \neq q} B_{s}^{(i)})] \\ &- \text{E}[d_{i}R_{q}^{(i)} \prod_{s \neq q} B_{s}^{(i)}]^{2} \bigg) \\ &= \sum_{i} \text{E}[d_{i}d_{i}^{*}] \text{E}[(R_{q}^{(i)})^{2}] \prod_{s \neq q} \text{E}[(B_{s}^{(i)})^{2}], \end{split}$$

by again utilizing that d_i has mean zero. We further assume $n_s = \beta \log n$ qubits in each subsystem, which implies that we can construct our ansatzes such that the gradients $R_q^{(i)}$ has zero mean and a variance which scales polynomially in the total number of qubits, n [14]. If $\prod_{s \neq q} \mathrm{E}[(B_s^{(i)})^2]$ also scales polynomially in n, it follows that the same can be said for the variance in Eq. 14. In order to find $\mathrm{E}[(B_s^{(i)})^2]$ we will utilize the following relation[17],

$$\begin{split} &\int d\mu(U) \mathrm{Tr}[UAU^{\dagger}B] \mathrm{Tr}[UCU^{\dagger}D] \\ &= \frac{\mathrm{Tr}[A]\mathrm{Tr}[B]\mathrm{Tr}[C]\mathrm{Tr}[D] + \mathrm{Tr}[AC]\mathrm{Tr}[BD]}{d^2 - 1} \\ &- \frac{\mathrm{Tr}[AC]\mathrm{Tr}[B]\mathrm{Tr}[D] + \mathrm{Tr}[A]\mathrm{Tr}[C]\mathrm{Tr}[BD]}{d(d^2 - 1)}, \end{split}$$

where d is the dimensionality of the system. Applied to our scenario this gives

$$\begin{split} & \int d\mu(U_s) \text{Tr}[U_s \rho U_s^{\dagger} W_s^{(i)}] \text{Tr}[U_s \rho U_s^{\dagger} W_s^{(i)}] \\ & = \frac{\text{Tr}[\rho]^2 \text{Tr}[W_s^{(i)}]^2 + \text{Tr}[\rho^2] \text{Tr}[(W_s^{(i)})^2]}{d^2 - 1} \\ & - \frac{\text{Tr}[\rho^2] \text{Tr}[W_s^{(i)}]^2 + \text{Tr}[\rho]^2 \text{Tr}[(W_s^{(i)})^2]}{d(d^2 - 1)}, \end{split}$$

where $d=2^{n_s}$. Assuming ρ is a pure state such that $\text{Tr}[\rho]=1$ and $\text{Tr}[\rho^2]=1$, and rearranging gives

$$\int d\mu(U_s) \text{Tr}[U_s \rho U_s^{\dagger} W_s^{(i)}] \text{Tr}[U_s \rho U_s^{\dagger} W_s^{(i)}]$$

$$= (d-1) \frac{\text{Tr}[W_s^{(i)}]^2 + \text{Tr}[(W_s^{(i)})^2]}{d(d^2-1)}.$$

Since $W_s^{(i)}$ is a Pauli-string, $(W_s^{(i)})^2=I$, and thus $\mathrm{Tr}[(W_s^{(i)})^2]=d$. Further, we have that $\mathrm{Tr}[\bigotimes_i A_i]=\prod_i \mathrm{Tr}[A_i]$. Since X,Y and Z have trace zero, this implies that any non-identity Pauli string will have $\mathrm{Tr}[W_s^{(i)}]^2=0$, while for identity Pauli-strings, $W_s^{(i)}=I$, we have $\mathrm{Tr}[W_s^{(i)}]^2=d^2$. We consider first the case when $W_s^{(i)}=I$. We then get

$$\begin{split} &\int d\mu(U_s) \mathrm{Tr}[U_s \rho U_s^\dagger W_s^{(i)}] \mathrm{Tr}[U_s \rho U_s^\dagger W_s^{(i)}] \\ &= \frac{(d-1)(d^2+d)}{d(d^2-1)} \\ &= \frac{(d-1)(d+1)}{(d^2-1)} \\ &= 1, \end{split}$$

which is expected from measurements of the identity operator on normalized states. When $W_s^{(i)}
eq I$ we get

$$\int d\mu(U_s) \operatorname{Tr}[U_s \rho U_s^{\dagger} W_s^{(i)}] \operatorname{Tr}[U_s \rho U_s^{\dagger} W_s^{(i)}]$$

$$= \frac{d(d-1)}{d(d^2-1)}$$

$$= \frac{d-1}{d^2-1}$$

$$= \frac{d-1}{(d-1)(d+1)}$$

$$= \frac{1}{d+1},$$

For $d = 2^{n_s} = 2^{\beta \log_2(n)} = n^{\beta}$ we thus have,

$$E\left[(B_s^{(i)})^2\right] = \begin{cases} 1 & \text{if } W_s^{(i)} = I\\ \frac{1}{n^{\beta}+1} & \text{otherwise.} \end{cases}$$

If $\bigotimes_{s\neq g}^S W_s^{(i)}$ acts non-trivially only on K of the subsystems, it follows that

$$\prod_{s \neq q}^{S} E[(B_s^{(i)})^2] = \frac{1}{(n^{\beta} + 1)^K},$$

which shows that terms of $D = \sum_p d_p \bigotimes_{s=1}^S W_s^p$ which are local to a constant subset of K of the subsystems have the appropriate scaling for the variance of the gradients.

3 Method

3.1 Ground state energy

In this section, we will introduce our Hamiltonian, as well as how the we construct our ansatz for the ground state.

3.1.1 The Hamiltonian

We will consider the 1D transverse-field Ising Hamiltonian with periodic boundary conditions. The Hamiltonian for n spins is given by,

$$H = -J\sum_{i=1}^{n} X_i X_{i+1} - h\sum_{i=1}^{n} Z_i,$$
(15)

where J is the interaction strength between neighbooring spins and h is the strength of the transverse field. The periodic boundary conditions imply $X_{n+1} = X_1$.

3.1.2 Subsystem unitaries

The parameterized quantum circuit (PQC) for each subsystem, that is $U_s(\vec{\theta}_s)$ in Eq. 10, is shown in Fig. 1.

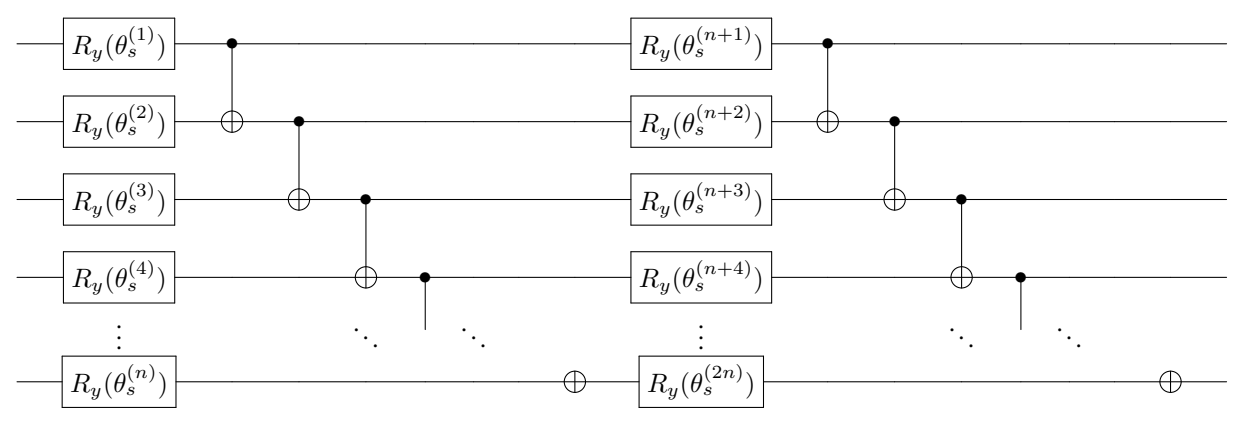


Figure 1: The parameterized quantum circuit for subsystem s. We apply R_y rotations to each qubit with an angle specified by the tunable parameters $\bar{\theta}_s^{(k)}$, followed by CNOT gates to produce entanglement. The procedure is done twice.

3.1.3 Global unitary

We aim to approximate the ground state energy of Eq. 15 for n = 4, 6, 8, 10, 12, 16 spins by defining the global unitary V according to Eq. 11. The Pauli-strings P_i utilized for the construction of V, along with the number of subsystems is shown in Tab. 1.

Table 1: Table showing the number of spins, n, subsystems S and the set of Pauli-strings $\{P_i\}$ utilized for our ground state approximation. We divided the qubits into equally sized subsystems of n/S qubits and the Pauli-strings are chosen to act along and between borders of these subsystems.

n	S	$\{P_i\}$	
4	2	$\{Z_2Y_3, Y_1Z_4\}$	
6	2	$\{Z_3Y_4, Y_1Z_6\}$	
8	2	$\{Z_3Y_4, Z_4Y_5, Z_5Y_6, Z_7Y_8, Y_1Z_8, Z_1Y_2\}$	
10	2	$\{Z_4Y_5, Z_5Y_6, Z_6Y_7, Z_9Y_{10}, Y_1Z_{10}, Z_1Y_2\}$	
12	3	$\{Z_3Y_4, Z_4Y_5, Z_5Y_6, Z_7Y_8, Z_8Y_9, Z_9Y_{10}, Z_{11}Y_{12}, Y_1Z_{12}, Z_1Y_2\}$	
16	4	$\{Z_3Y_4, Z_4Y_5, Z_5Y_6, Z_7Y_8, Z_8Y_9, Z_9Y_{10}, Z_{11}Y_{12}, Z_{12}Y_{13}, Z_{13}Y_{14}, Z_{15}Y_{16}, Y_1Z_{16}, Z_1Y_2\}$	

Division of the qubits into equally sized subsystems of n/S qubits and this choice of Pauli-strings ensures V to act along and between borders of these subsystems to capture longer-range correlations.

3.2 Supervised learning

In this section, we will introduce the dataset and the structure of the model utilized for classification of handwritten digits.

3.2.1 Dataset

We will perform supervised learning on the digits dataset, which is the classification of handwritten digits from 0 to 9. Each sample is an 8 by 8 pixel image, which will require a 64 qubit quantum computer when encoding each pixel into its respective qubit. We will, similarly to [13], reduce this to a binary classification task of the numbers 3 and 6. The task will be performed on a simulation of a 8 qubit quantum computer and $\vec{x}^{(s)}$ in eq. 6 will thus contain the 8 pixels of the s'th column of the image. The pixels will be scaled to be in the range $[0,\pi]$ to serve as rotational angles in the parameterized ansatzes. The total number of samples in the dataset is 364, and these samples will be divided into 182 samples for training the model, 91 samples for validation and 91 samples for testing.

3.2.2 Ansatz

The eight-qubit ansatzes corresponding to the unitaries U_s in Eq. 6 is shown in Figs. 2 and 3.

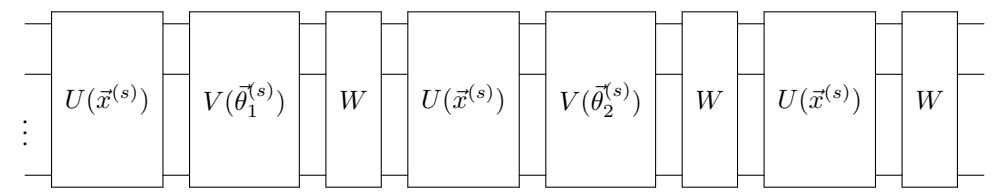


Figure 2: The ansatz employed for the digits dataset. We utilize a data re-uploading scheme [18] with alternating layers of single-qubit rotations and entangling gates. The different components are explicitly written out in figure 3.

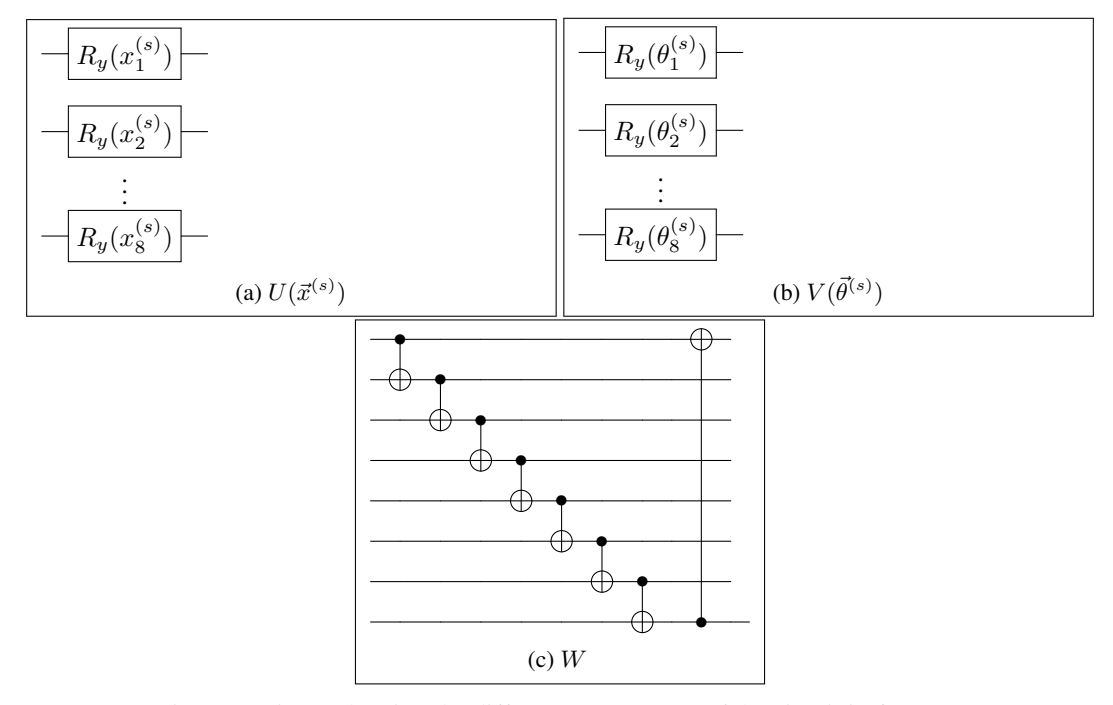


Figure 3: Figure showing the different components of the circuit in figure 2.

For the ansatzes, we apply a data re-uploading scheme to increase the expressiveness of our PQC. This is done by applying our feature encoding, $U(\vec{x}^{(s)})$ (see fig 3 (a)), at several occasions in the ansatzes in fig 2. It has been shown that the use this technique with only a single qubit can construct a universal quantum classifier [18]. The application of

 $V(\vec{\theta}^{(s)})$ (see fig 3 (b)) encodes the tunable parameters of our model. This is done at two occasions with two different sets of parameters, $\vec{\theta}_1^{(s)}$ and $\vec{\theta}_2^{(s)}$, in order to further increase the expressiveness of the model. Since we are dealing with 8 subspaces, the total number of parameters for our ansatzes is $8 \cdot 16 = 128$. The applications of CNOT gates, W (see fig 3 (c)), is done to generate entanglement. The final CNOT in W is included to hopefully distribute the data more evenly across the qubits. If this kind of connectivety is not available on the quantum device, one could omit the final CNOT and for example alternate between CNOTs on following and preceding qubits instead.

3.2.3 Observable

The observable for our task will alternate between measuring correlations between the first qubits in subsets s and s+1, and correlations between the final qubits in subsets s+1 and s+2. That is

$$D^{(s,s+1)} = \begin{cases} \sum_{p} d_{p}^{(s)} \sigma_{1,p}^{(s)} \sigma_{1,p}^{(s+1)}, & \text{if } s \mod 2 = 1\\ \sum_{p} d_{p}^{(s)} \sigma_{8,p}^{(s)} \sigma_{8,p}^{(s+1)}, & \text{otherwise,} \end{cases}$$
(16)

where $s \in \{1, 2, \dots, 7\}$ and $\sigma_{j,p}^{(s)}$ are one of the operators the Pauli basis, acting on the j'th qubit in subset s. We will restrict the coefficients $d_p^{(s)}$ to real scalars since our model outputs are real. If n_b operators in the Pauli-basis is utilized in the construction of this observable, we require a total of $7 \cdot 2n_b$ measurements and $7 \cdot 2^{n_b}$ coefficients to calculate our model output.

4 Results

We will now present the results for the approximation of the ground state energy of the 1D transverse-field Ising Hamiltonian, as well as for the classification of handwritten digits. We refer the reader to the Methods section 3 for further details on how the models were configured.

4.1 Ground state energy

As detailed in section 3.1, the quantum system we will test out the method on is the 1D transverse-field Ising model with periodic boundary conditions, given by Eq. 15. We aim to approximate the ground state energy for n = 4, 6, 8, 10, 12, 16 spins and we define the global unitary V according to Eq. 11. The Pauli-strings P_i utilized for the construction of V, along with the number of subsystems is shown in Tab. 1.

The parameters of the PQC, $\vec{\theta}_s$, as well as the coefficients of V, that is c_i , are randomly initialized. The energy is then minimized by calculating the energy gradients in Eqs. 12 and 13, and utilizing gradient descent with the ADAM optimizer[19]. This is done with a learning rate of 0.1 and 200 training steps for every system. The results are compared with the exact diagonalization of the Hamiltonian in Eq. 15, as shown in Fig. 4.

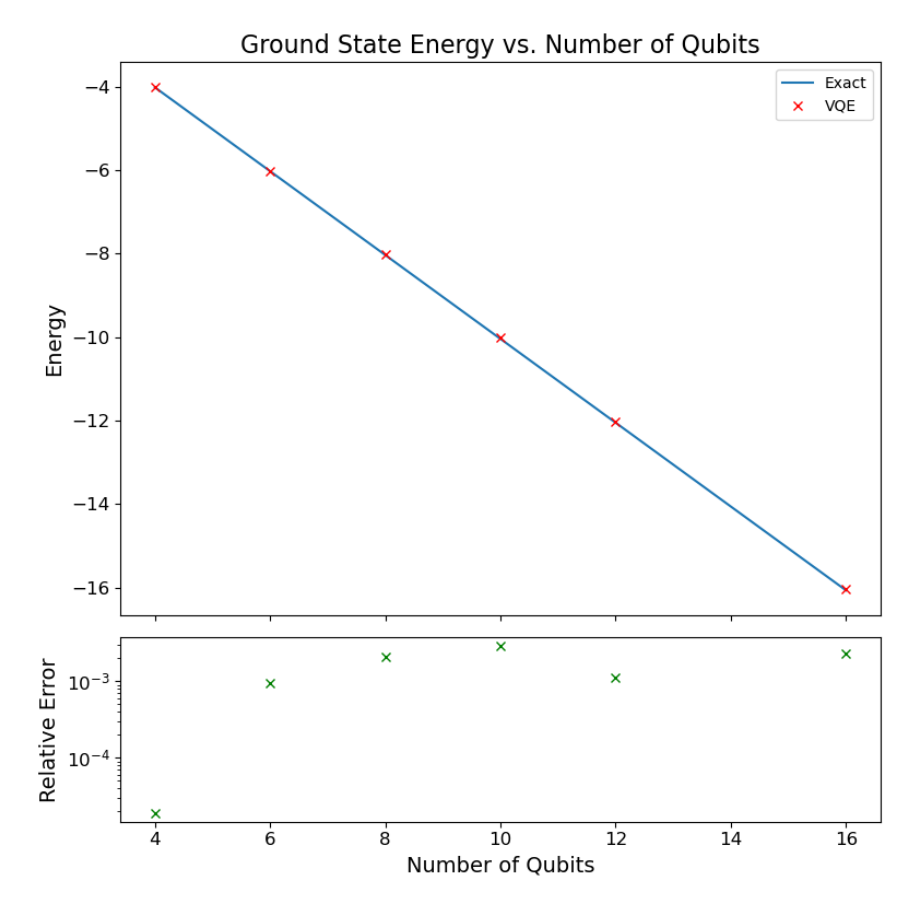


Figure 4: The exact ground state energy of the 1D transverse-field Ising model is compared with our approximation for n number of spins/qubits. The top plot compares the achieved energies, while the bottom plot shows the relative error $(E_{\text{VOE}} - E_0)/E_0$ between the ground state energy E_0 and our approximation E_G .

The results of Fig. 4 demonstrates the capability to approximate the ground state energy with a relative error within the order of 0.1% for all the tested numbers of qubits.

4.2 Supervised learning

Following the model structure in section 3.2, we trained two different instances of our model. First we utilized the full Pauli-basis, $\{I, \sigma_x, \sigma_y, \sigma_z\}$ in the construction of the observables in eq. 16. Since each of these observables only act on two subsets and one qubit in each, one evaluation of the model corresponds to 56 expectation values and we require 112 coefficients. Since we have eight subsystems with 16 trainable rotational angles each, we have a total of 240 trainable parameters in this model. For the second instance of the model, we utilized a truncated basis consisting of only the operators $\{I, \sigma_x\}$. One model evaluation corresponds to a total of 28 expectation values and we require 28 coefficients. This leads to a total of 156 trainable parameters. For both of these models, the mean squared error (MSE) was chosen as the loss function and the models were trained for 400 epochs using the Adam optimizer with learning rate 0.1.

Figure 5 shows the training and validation MSE as a function of the epoch for both models. For both models, we see a rapid decrease of the training loss before seemingly converging towards a stable value. The validation loss also decreases similarly to the training loss in the early training stages, suggesting that the model generalizes to unseen data. Eventually, the validation loss starts to increase for both models, suggesting that overfitting might be occurring at some state. The final models were thus chosen from the epoch with the smallest MSE on the validation data. The resulting models were then applied on the remaining test data. The results are shown in table 2.

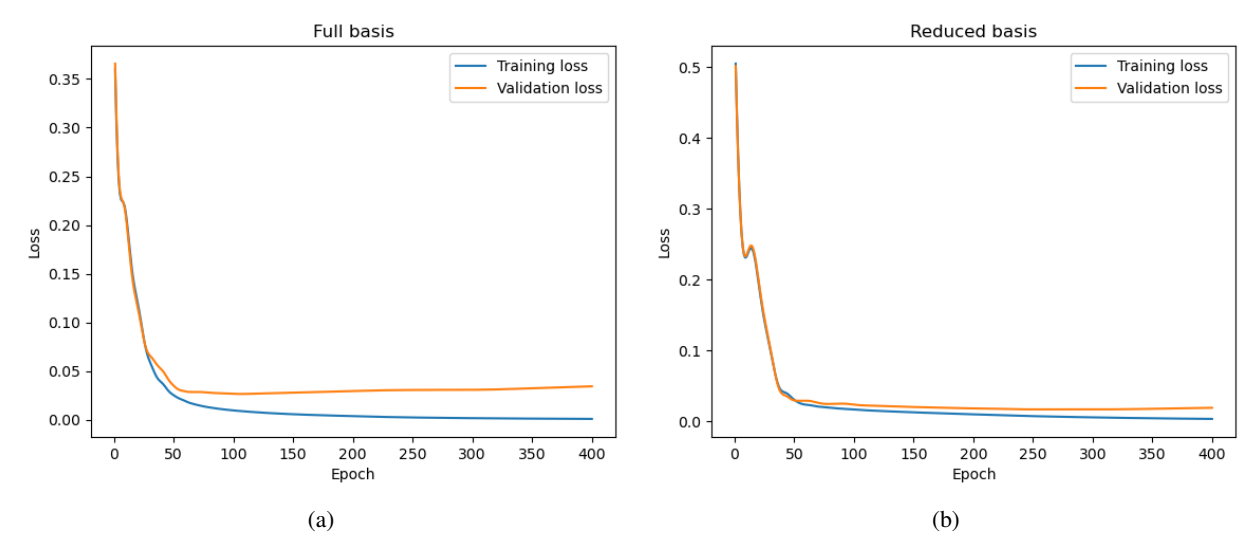


Figure 5: Shows the MSE loss as a function of epoch for the training and validation data for two different models. For both models, the final parameters corresponds to the parameters that minimized the validation loss. Figure (a) shows the loss when utilizing the full basis, $\{I, \sigma_x, \sigma_y, \sigma_z\}$ to construct the observables in eq. 16. For this case, the validation loss was minimized at epoch 105. Figure (b) shows the loss for when the reduced basis, $\{I, \sigma_x\}$ was utilized to construct the observables. The validation loss was minimized at epoch 250.

Table 2: The MSE and accuracy for the model utilizing the full basis (FB) of Pauli operators and the reduced basis (RB) consisting of $\sigma_a \in \{I, \sigma_x\}$.

	Accuracy	MSE
	FB/RB	FB/RB
Training	1.0000 / 1.0000	0.0090 / 0.0076
Validation	0.9890 / 1.0000	0.0265 / 0.0171
Testing	0.9780 / 1.0000	0.0304 / 0.0250

Interestingly, the model utilizing the reduced basis is generalizing to unseen data better than the model with the full basis. This might be due to the basis reduction acting as a form of regularization, preventing overfitting. However, only one instance of each model have been trained, so these results might be coincidental.

5 Conclusion

In conclusion, our study presents an approach for evaluating the expectation values of specific quantum states by decomposing the problem into smaller components to be evaluated on smaller quantum computers. The problem uses well-known techniques such as the measurement of expectation values of Pauli-strings and the parameter-shift rule[15], and can be tailored to mitigate the problem of barren plateaus. The approach can be utilized in the context of ground state energy approximation and also for quantum machine learning, which was demonstrated by applying the method to the 1D transverse-field Ising model with periodic boundary conditions, as well as for the digits dataset. For the ground state approximation, we achieved a relative error within the order of 0.1% for all the tested systems sizes of n=2,4,6,8,10,12,16 spins. For the digits dataset, the classification between the digits 3 and 6 showed that our model was able to generalize to unseen data with 100% accuracy.

Looking ahead, we would like to apply the method to diverse quantum systems and datasets to assess its generalizability. Additionally, we would like to investigate the performance of our method in the presence of noise akin to currently available quantum devices. While the aforementioned studies are crucial for evaluating the potential for practical applications, this paper highlights the promise of our method and the potential in using small quantum devices for high-dimensional ground state approximation and machine learning tasks.

References

- [1] David Deutsch and Richard Jozsa. Rapid solution of problems by quantum computation. *Proceedings of the Royal Society of London. Series A: Mathematical and Physical Sciences*, 439(1907):553–558, 1992. doi:10.1098/rspa.1992.0167. URL https://royalsocietypublishing.org/doi/abs/10.1098/rspa.1992.0167.
- [2] P.W. Shor. Algorithms for quantum computation: discrete logarithms and factoring. In *Proceedings 35th Annual Symposium on Foundations of Computer Science*, pages 124–134, 1994. doi:10.1109/SFCS.1994.365700.
- [3] Patrick Rebentrost, Masoud Mohseni, and Seth Lloyd. Quantum support vector machine for big data classification. *Phys. Rev. Lett.*, 113:130503, Sep 2014. doi:10.1103/PhysRevLett.113.130503. URL https://link.aps.org/doi/10.1103/PhysRevLett.113.130503.
- [4] Seth Lloyd, Masoud Mohseni, and Patrick Rebentrost. Quantum principal component analysis. *Nature Physics*, 10(9):631–633, 2014. doi:10.1038/nphys3029. URL https://doi.org/10.1038/nphys3029.
- [5] Nathan Wiebe, Ashish Kapoor, and Krysta M. Svore. Quantum algorithms for nearest-neighbor methods for supervised and unsupervised learning. *Quantum Info. Comput.*, 15(3–4):316–356, mar 2015. ISSN 1533-7146.
- [6] John Preskill. Quantum Computing in the NISQ era and beyond. *Quantum*, 2:79, August 2018. ISSN 2521-327X. doi:10.22331/q-2018-08-06-79. URL https://doi.org/10.22331/q-2018-08-06-79.
- [7] Marcello Benedetti, Erika Lloyd, Stefan Sack, and Mattia Fiorentini. Parameterized quantum circuits as machine learning models. *Quantum Science and Technology*, 4(4):043001, nov 2019. doi:10.1088/2058-9565/ab4eb5. URL https://dx.doi.org/10.1088/2058-9565/ab4eb5.
- [8] Smita Paira, Sourabh Chandra, Sk Alam, and Partha Dey. A review report on divide and conquer sorting algorithm. 11 2014.
- [9] Michael Ian Shamos and Dan Hoey. Geometric intersection problems. In 17th Annual Symposium on Foundations of Computer Science (sfcs 1976), pages 208–215, 1976. doi:10.1109/SFCS.1976.16.
- [10] V. STRASSEN. Gaussian elimination is not optimal. *Numerische Mathematik*, 13:354–356, 1969. URL http://eudml.org/doc/131927.
- [11] Sergey Bravyi, Graeme Smith, and John A. Smolin. Trading classical and quantum computational resources. *Phys. Rev. X*, 6:021043, Jun 2016. doi:10.1103/PhysRevX.6.021043. URL https://link.aps.org/doi/10.1103/PhysRevX.6.021043.
- [12] Keisuke Fujii, Kaoru Mizuta, Hiroshi Ueda, Kosuke Mitarai, Wataru Mizukami, and Yuya O. Nakagawa. Deep variational quantum eigensolver: A divide-and-conquer method for solving a larger problem with smaller size quantum computers. *PRX Quantum*, 3:010346, Mar 2022. doi:10.1103/PRXQuantum.3.010346. URL https://link.aps.org/doi/10.1103/PRXQuantum.3.010346.
- [13] Simon C. Marshall, Casper Gyurik, and Vedran Dunjko. High Dimensional Quantum Machine Learning With Small Quantum Computers. *Quantum*, 7:1078, August 2023. ISSN 2521-327X. doi:10.22331/q-2023-08-09-1078. URL https://doi.org/10.22331/q-2023-08-09-1078.
- [14] Cenk Tüysüz, Giuseppe Clemente, Arianna Crippa, Tobias Hartung, Stefan Kühn, and Karl Jansen. Classical splitting of parametrized quantum circuits. *Quantum Machine Intelligence*, 5(2):34, 2023. doi:10.1007/s42484-023-00118-z. URL https://doi.org/10.1007/s42484-023-00118-z.
- [15] Maria Schuld, Ville Bergholm, Christian Gogolin, Josh Izaac, and Nathan Killoran. Evaluating analytic gradients on quantum hardware. *Phys. Rev. A*, 99:032331, Mar 2019. doi:10.1103/PhysRevA.99.032331. URL https://link.aps.org/doi/10.1103/PhysRevA.99.032331.
- [16] Jarrod R. McClean, Sergio Boixo, Vadim N. Smelyanskiy, Ryan Babbush, and Hartmut Neven. Barren plateaus in quantum neural network training landscapes. *Nature Communications*, 9(1):4812, 2018. doi:10.1038/s41467-018-07090-4. URL https://doi.org/10.1038/s41467-018-07090-4.
- [17] M. Cerezo, Akira Sone, Tyler Volkoff, Lukasz Cincio, and Patrick J. Coles. Cost function dependent barren plateaus in shallow parametrized quantum circuits. *Nature Communications*, 12(1):1791, 2021. doi:10.1038/s41467-021-21728-w. URL https://doi.org/10.1038/s41467-021-21728-w.
- [18] Adrián Pérez-Salinas, Alba Cervera-Lierta, Elies Gil-Fuster, and José I. Latorre. Data re-uploading for a universal quantum classifier. *Quantum*, 4:226, February 2020. ISSN 2521-327X. doi:10.22331/q-2020-02-06-226. URL https://doi.org/10.22331/q-2020-02-06-226.
- [19] Diederik P. Kingma and Jimmy Ba. Adam: A method for stochastic optimization, 2014. URL https://arxiv.org/abs/1412.6980.